CANCER BIOTHERAPY & RADIOPHARMACEUTICALS
Volume 20, Number 5, 2005

Intraperitoneal Radioimmunotherapy with a Humanized Anti-TAG-72 (CC49) Antibody with a Deleted CH2 Region

Buck E. Rogers,[1] Peter L. Roberson,[3] Sui Shen,[1] M.B. Khazaeli,[2] Mark Carpenter,[3] Shigeru Yokoyama,[3] Martin W. Brechbiel,[4] Albert F. LoBuglio,[2] and Donald J. Buchsbaum[1]
Departments of [1]Radiation Oncology and [2]Medicine, University of Alabama at Birmingham, Birmingham, AL
[3]Department of Radiation Oncology, University of Michigan, Ann Arbor, MI
[4]Radioimmune and Inorganic Chemistry Section, National Cancer Institute, National Institutes of Health, Bethesda, MD

ABSTRACT

The application of intraperitoneal (i.p.) radioimmunotherapy to treat i.p. tumor loci *has been limited by bone marrow toxicity secondary to circulating radiolabeled antibodies. The generation of novel genetically engineered monoclonal antibodies, which can achieve high tumor uptake and rapid blood clearance, should enhance the therapeutic index of i.p. radioimmunotherapy. In this regard, a novel humanized anti-TAG-72 monoclonal antibody with a deleted CH2 region (HuCC49ΔCH2) has been described, which localized well to subcutaneous xenograft tumors and had a rapid plasma clearance. The aim of this study was to examine the characteristics of this radiolabeled reagent when administered through the i.p. route in mice bearing i.p. tumor (LS174T). The ΔCH2 molecule and intact humanized CC49 (HuCC49) monoclonal antibody were conjugated to PA-DOTA and radiolabeled with ^{177}Lu. Both molecules retained high-affinity binding to TAG-72 positive LS174T tumor cells* in vitro. *The radiolabeled ΔCH2 molecule had a modest decrease in tumor localization, as compared to the intact molecule when administered i.p. to tumor-bearing mice and a dramatically shorter plasma disappearance $T_{1/2}$ at 2.7 hours compared to 61.2 hours for the intact antibody. The radiolabeled ΔCH2 molecule thus had very high tumor:blood ratios. Using an ^{131}I-labeled system, the maximum tolerated dose of ΔCH2 was >3× that of intact HuCC49. Autoradiography of tumors showed low radiation dose rates at tumor centers early (1 and 4 hours), as compared to higher dose rates at tumor periphery but a more uniform distribution by 24 hours. Dose-rate distributions were similar for both reagents. Animals bearing LS174T i.p. tumors were treated with 300 μCi of ^{177}Lu-labeled ΔCH2 or intact HuCC49 by i.p. route daily × 3. The ^{177}Lu-ΔCH2 molecule mediated an increase in median survival compared to controls (67.5 ± 7.5 days versus controls of 32 ± 3.3) while the same dose of ^{177}Lu-HuCC49 produced early toxic deaths. These studies suggest that i.p. radioimmunotherapy using radiolabeled HuCC49ΔCH2 should allow higher radiation doses to be administered with less marrow toxicity and potentially improved efficacy.*

Key words: TAG-72, Lutetium-177, CC49, dosimetry, pharmacokinetics, therapy

Address reprint requests to: Donald J. Buchsbaum; Department of Radiation Oncology, University of Alabama at Birmingham; 1824 6th Avenue South, WTI 674, Birmingham, AL 35294; Tel.: (205) 934-7077; Fax: (205) 975-7060
E-mail: djb@uab.edu
This work was supported by NIH grant 1 P50 CA83591.

INTRODUCTION

Radiolabeled monoclonal antibodies (mAbs) have been used clinically for the diagnosis and treatment of cancer.[1–5] In general, ^{131}I has been the radioisotope most frequently used for radio-

labeling, although various radiometals (^{111}In, ^{99m}Tc, ^{90}Y, ^{177}Lu, $^{64/67}$Cu, $^{186/188}$Re) have also been utilized with the advent of bifunctional chelating agents capable of forming high-stability complexes with these metals. Radiolabeling mAbs with radiometals has advantages over radiolabeling with ^{131}I including more favorable beta and photon energy characteristics and lack of *in vivo* deiodination. However, problems still exist with radiometal-labeled intact murine mAbs including the human antimouse antibody (HAMA) response and myelotoxicity resulting from slow clearance of the radiolabeled mAbs from the serum. For diagnostic imaging, the slow serum clearance also requires more time between radiolabeled mAb administration and imaging in order to achieve higher target to background ratios.

Genetically engineered mAbs have been utilized to address the problem of HAMA responses in patients.[6] Chimeric mAbs (cmAbs) consist of variable regions from the native murine mAbs attached to human constant regions, while for humanized mAbs (HumAbs), only the antigen-binding complementarity-determining region are from the native murine mAbs with the remainder of the framework being human. These engineered mAbs have been shown to reduce the immune response in patients[6,7] while maintaining a high affinity for the target antigen. However, a drawback of these mAbs is that their clearance from serum in humans is even slower than the corresponding murine mAbs.[6,7] Thus, although cmAbs and HumAbs address the problem of HAMA responses in patients, they may lead to even greater myelotoxicity.

One approach toward reducing myelotoxicity is to increase the serum clearance of radiolabeled mAbs by decreasing their size. In this regard, it has been shown that radiolabeled F(ab′)$_2$ and Fab′ mAb fragments clear from serum of mice and humans more rapidly than intact mAbs.[8] Also, genetically engineered single-chain variable region mAbs (sFvs) have been radiolabeled and shown to clear from serum of mice more rapidly than intact mAbs.[9–11] Drawbacks of these radiolabeled fragments include increased radiation dose to the kidneys (the primary clearance organ), lower antigen affinity of the monovalent Fab′ and sFv molecules, and decreased radiation dose delivered to the tumor resulting from their rapid serum clearance. However, a potential advantage is that they show more uniform intratumor penetration, depending on the affinity of the sFv for the antigen.[12–14] Other mAbs and HumAbs with reduced size have been engineered in which the CH1 or CH2 domain of the constant region of the mAb has been deleted and replaced with a peptide linker.[15] Serum clearance of radiolabeled mAbs with the CH2 domain deleted was more rapid in mice than the serum clearance of intact radiolabeled mAbs. It has been postulated that this occurs not only because of the difference in size between the two molecules but because of removal of the glycosylation site present in the CH2 region, which may facilitate receptor-mediated clearance through the liver.[15] The radiolabeled CH2-deleted mAbs have demonstrated good tumor uptake when compared to other low-molecular-weight fragments and have not shown the high kidney uptake observed with these constructs. Thus, the utilization of a HumAb with the CH2 region deleted is a logical choice for use in diagnosis and therapy based on its potentially low immunogenicity, rapid blood clearance, and good tumor localization.

CC49 is a second-generation murine mAb reactive with the TAG-72 antigen, which is found on a variety of adenocarcinomas, including pancreatic, breast, colorectal, prostate, and ovarian.[16,17] CC49 has a higher antigen-binding affinity for TAG-72 than its parent mAb, B72.3, and has been radiolabeled with ^{131}I, ^{90}Y, and ^{177}Lu for use in phase I/II clinical therapy trials with encouraging results.[18–24] Clinical trials at our institution have utilized ^{177}Lu-labeled murine CC49 for the treatment of recurrent ovarian cancer limited to the peritoneal cavity.[21,24] Lutetium-177 has a 6.7-day half-life with a maximum β emission of 497 keV and relatively low-energy γ emissions that can be used for imaging but deliver less radiation dose to personnel than ^{131}I. ^{131}I has an 8-day half-life, a maximum β emission of 810 keV, and an imageable γ-emission. ^{90}Y has a 2.7-day half-life and a higher maximum β emission of 2.3 MeV but is unsuitable for quantitative imaging. Many groups are utilizing ^{111}In biodistribution data to predict dose for ^{90}Y administrations. Our ovarian cancer clinical studies were conducted using i.p. administration of the radiolabeled mAb, as it has been demonstrated that this route of administration leads to higher tumor localization than (intravenous) i.v. administration for the treatment of disease limited to the peritoneal cavity.[25] Hematologic toxicity was dose limiting in these studies, in part owing to the relatively long plasma $T_{1/2}$ of murine CC49 (50 hours). HAMA responses were observed in the majority of patients.[21,24] Therefore, utiliza-

tion of radiolabeled HuCC49ΔCH2, which has been humanized and CH2-deleted, should address these limitations and may result in even greater therapeutic efficacy in clinical trials.

Chimeric mAbs of CC49 (cCC49) that contain CH1 and CH2 deletions (cCC49ΔCH1 and cCC49ΔCH2, respectively) have been produced, radiolabeled, and evaluated for biodistribution in mice.[15] These studies demonstrated that serum clearance of the radiolabeled cCC49 and cCC49ΔCH1 mAbs was similar, while the serum clearance of radiolabeled cCC49ΔCH2 was significantly faster.[15] The humanized intact CC49 (HuCC49) and humanized CH2 deleted CC49 (HuCC49ΔCH2) have also been produced.[26,27] The HuCC49 and HuCC49ΔCH2 were radioiodinated and evaluated for biodistribution in mice bearing subcutaneous tumors.[26,27] The results showed that the radioiodinated HuCC49ΔCH2 cleared more rapidly from the serum than the radioiodinated HuCC49 after i.p. or i.v. administration. The tumor to normal tissue ratios were greater (except for spleen) for the radioiodinated HuCC49ΔCH2 than the radioiodinated HuCC49 at all times measured. Thus, radioiodinated HuCC49ΔCH2 was shown to have a favorable biodistribution after i.v. or i.p. administration in mice bearing subcutaneous tumors when compared to radioiodinated HuCC49. Therefore, evaluation of HuCC49ΔCH2 radiolabeled with ^{177}Lu in the context of peritoneal disease and regional administration is of interest.

In this study, we describe the radiolabeling of HuCC49 and HuCC49ΔCH2 with ^{177}Lu. The ^{177}Lu-labeled HuCC49 and HuCC49ΔCH2 were compared in mice bearing i.p. colon cancer xenografts by tissue biodistribution and pharmacokinetic analysis. Also, intratumor uptake of ^{177}Lu-labeled HuCC49 and HuCC49ΔCH2 was determined by autoradiography. Absorbed radiation doses delivered to the tumor and normal tissues were determined. Intraperitoneal therapy with ^{177}Lu radiolabeled antibodies (ΔCH2 and intact) was also studied. The aim of these studies was to determine the feasibility of using ^{177}Lu-labeled HuCC49ΔCH2 in clinical trials for the treatment of peritoneal ovarian cancer.

MATERIALS AND METHODS

Cell Line and Antibodies

The LS174T human colon cancer cell line was obtained from the American Type Culture Collection (Rockville, MD) and cultured in Eagles Minimum Essential Medium containing 10% fetal bovine serum, 1% L-glutamine, and 1% nonessential amino acids at 37°C in a humidified atmosphere with 5% CO_2. The HuCC49 and HuCC49ΔCH2 mAbs were prepared as previously described[26,27] and stored at −70°C until use.

Radiolabeling with ^{131}I and ^{177}Lu

HuCC49 and HuCC49ΔCH2 were labeled with ^{131}I using our previously described procedure to a specific activity of 6 mCi/mg.[28] The bifunctional chelating agent PA-DOTA-NCS was synthesized as previously described[29] and conjugated to HuCC49 and HuCC49ΔCH2. Briefly, the PA-DOTA-NCS was diluted to 0.5 mg/mL in 0.1 M H_3BO_4 and added to HuCC49 and HuCC49ΔCH2 (in the same buffer) in a 6:1 molar ratio, such that the final concentration of HuCC49 was ~25 mM and the final concentration of HuCC49ΔCH2 was ~50 mM. The reaction mixtures were then incubated at 37°C for 4 hours and purified using a Centricon 30 concentrator (Amicon Inc.; Beverly, MA). The samples were added to the Centricon 30, diluted to 2.0 mL with 0.1 M NH_4OAc, pH 5.5, and centrifuged. This was repeated three times, the conjugates collected, and stored at 4°C until needed. $^{177}LuCl_3$ (initial specific activity ~4000 Ci/mmol) was produced and purified at the University of Missouri—Columbia Research Reactor (Columbia, MO). The $^{177}LuCl_3$ was diluted 10-fold with 0.1 M NH_4OAc, pH 5.5, and added to the PA-DOTA-NCS conjugates. The reaction mixtures were incubated for 30 minutes at 37°C and purified using a BioSpin 6 chromatography column (Bio-Rad Laboratories; Hercules, CA) equilibrated with 0.1 M NH_4OAc, pH 5.5. The purity of the radiolabeled mAbs was determined by size-exclusion high-performance liquid chromatography (HPLC). HPLC samples were run on a Hydropore SEC 83-S13-C5 column (Rainin Instrument Co.; Emeryville, CA) using a Bio-Rad HPLC Pump Model 1330 (Bio-Rad Laboratories) and an isocratic buffer of 10 mM Na_2HPO_4, 300 mM NaCl, and 10% DMSO at a flow rate of 1 mL/minute.

Competitive Inhibition Assay

LS174T cells were harvested and suspended in cold PBS at a concentration of 1×10^7 cells/mL. The cells were aliquoted (100 μL) into poly-

styrene tubes in triplicate followed by addition of 100 μL of ^{177}Lu-PA-DOTA-HuCC49 or ^{177}Lu-PA-DOTA-HuCC49ΔC_H2 (0.15–0.33 nM). Various concentrations (10 μL; 0.2 pM–2.0 μM) of unlabeled PA-DOTA-HuCC49 or PA-DOTA-HuCC49ΔC_H2 were added as inhibitors. The solutions were mixed at 4°C for 1 hour, rinsed with PBS, and centrifuged at 1700 $\times$ g for 10 minutes. The supernatant was removed and the cells counted in a gamma counter to determine the amount of bound radioactivity. The data were analyzed using the GraphPad Prism software (San Diego, CA).

Biodistribution and Pharmacokinetic Analysis

Experiments were performed in 4–5-week old athymic nu/nu nude mice (National Cancer Institute Frederick Research Laboratory; Frederick, MD) implanted i.p. with 1×10^8 LS174T cells followed by an i.p. injection of 2 μCi ^{177}Lu-PA-DOTA-HuCC49 or ^{177}Lu-PA-DOTA-HuCC49ΔC_H2 8 days after tumor cell inoculation. Biodistribution was performed with groups of 4–5 mice killed 4 and 24 hours after injection of the radiolabeled antibodies. The blood, lungs, liver, spleen, kidney, bone, muscle, uterus, pancreas, and tumor were removed and weighed, and the radioactivity counted in a gamma counter to determine the percent injected dose per gram of tissue (%ID/g). A separate pharmacokinetic experiment was performed in which groups of 4–5 mice were killed 0.5, 1, 4, 12, 24, and 48 hours after injection of the radiolabeled antibodies. These data were used to determine the C_{max}, area under the curve (AUC), $T_{1/2}$ and dosimetry of ^{177}Lu-PA-DOTA-HuCC49 or ^{177}Lu-PA-DOTA-HuCC49ΔC_H2 in tumor, blood, liver, and kidney in this animal model.

Statistical Analysis

The sample mean and standard error for %ID/g were calculated at each time point for each group and each tissue type (blood and tumor, liver and kidney) so as to examine distribution and variation of time concentration of the radiolabeled 5 mAbs. The pharmacokinetic parameters were estimated using the nonlinear regression procedure (NLIN) of the Statistical Analysis System (SAS®).[30] Both one and two compartment models, including an absorption term, were fit for each tissue and treatment condition. Because of the added complication of only having observed a few time points subsequent to the absorption phase, a two-compartment model was selected over a one-compartment only if the extra exponential term in this model provided statistically significant improvement over the one-compartment model. In fact, there was only one case in which a two-compartment model was selected over a one-compartment model, the ^{177}Lu-PA-DOTA-HuCC49 in the blood model. Elimination ($T_{1/2el}$) and absorption ($T_{1/2ab}$) half-lives, AUC, T_{max}, and C_{max} were estimated using the parameter estimates from the selected compartmental model.

The Wilcoxon two-sample test was used to compare mean values of corresponding tissues (blood, lungs, liver, spleen, kidney, bone, muscle, uterus, pancreas, and tumor) of ^{177}Lu-PA-DOTA-HuCC49 with ^{177}Lu-PA-DOTA-HuCC49ΔC_H2 at 4 and 24 hours.

Autoradiography

Tumors were resected and serially sectioned at 1, 4, 24, and 48 hours post injection with ^{177}Lu-PA-DOTA-HuCC49 or ^{177}Lu-PA-DOTA-HuCC49ΔC_H2 monoclonal antibody. Between 5 and 24 (average 16) sections were retained per tumor for autoradiography. The typical interval between sections was 340 μm. Section thickness was 16 μm. Tumor sections were air-dried and placed on film (Super RX 20.3 $\times$ 25.4 cm, FujiFilm; Stamford, CT) and/or phosphor screen (BAS-MS Imaging Plates 20 $\times$ 25 cm with BAS-1800 scanner, FujiFilm; Stamford, CT) for autoradiography. Section images from film were digitized at 100 μm resolution using a laser densitometer (Lumysis; Sunnyvale, CA). Phosphor imager pixel resolution was set to 100 μm. Film and phosphor screen responses were measured using gel samples with known activity density, which were sectioned and imaged along with the tumor sections.

Digitized section images were used to generate tumor surface and activity distribution by reconstructing the tumor activity density in three dimensions, as previously described.[31] A linear interpolation of activity density information was used to fill the three-dimensional (3-D) activity density matrix. Surface descriptions were created using autocontouring of the images and checked using optically scanned images of the section slides. Three-dimensional activity density dose-rate calculations were performed using a point kernel for ^{177}Lu (WV Prestwich, private com-

munication). A voxel kernel was derived by distributing point kernels in the voxel volume. The voxel kernel was folded with the activity density matrix by Fast Fourier analysis. Some tumor matrices were summed to a 0.2-mm cubic voxel for the dose-rate calculation owing to limitations on matrix size for the Fast Fourier calculations. The dose-rate information was used to prepare radial histograms describing the variation in dose rate as a function of distance from the tumor center of mass to the tumor surface.

Radiation Dosimetry

The concentrations of ^{177}Lu-PA-DOTA-HuCC49 and ^{177}Lu-PA-DOTA-HuCC49ΔCH2 at each time point were expressed as %ID/g. Median cumulated activities were determined by integrated area under the time activity curve using the median value of the group of mice at each time point within 48 hours. Median cumulated activities per unit of mass per injected dose (μCi-h/g-μCi) were used to calculate radiation doses. Because ^{177}Lu is predominated by nonpenetrating radiation, radiation-absorbed dose from ^{177}Lu in target tissue itself was considered in the marrow, liver, kidney, and tumor-dose calculation:

$$\text{Dose} = \Sigma \phi_{np}\ \Delta_{np}\ \tilde{A}/m$$

where ϕ_{np} is the absorbed fraction for nonpenetrating emission in the target tissue, Δ_{np} is the equilibrium dose constant for nonpenetrating emission, and $\tilde{A}$ is the cumulated activity in the target tissue.

Radiation dose to the marrow was calculated from the concentration of ^{177}Lu in the blood. The ratio of marrow $\tilde{A}$ to that of blood was assumed to be 0.25.[32] The energy deposition to mouse marrow were determined using a mouse model considering mouse marrow in a set of slab, spherical, and cylindrical geometries.[33,34] The self-absorbed fractions ϕ_{np} for marrow to marrow were determined using beta dose-point kernels derived from medical internal radiation dose (MIRD) 7.[35] Tumor masses ranged from 60 to 900 mg, with a median mass of 235 mg. The absorbed fraction for liver mass of 1 g and kidney mass of 130 mg was also calculated.

The maximum tolerated dose (MTD) of a single i.p. injection of ^{131}I-labeled HuCC49ΔCH2 and HuCC49 were determined in groups of 8 normal Balb/c nude mice, based on a loss of animal weight of less than 15% and no deaths.

Therapy Studies

Athymic nu/nu nude female mice, 6–8 weeks old, were implanted i.p. with 5×10^7 LS174T cells. At 7 days after inoculation, animals received 300 μCi of either ^{177}Lu-labeled HuCC49 or ^{177}Lu-HuCC49ΔCH2 by i.p. injection three times daily on consecutive days. Survival of each animal was checked daily, and the day of death was recorded as the animal's survival time. The resulting survival (time, in days, until death) data where analyzed. Kaplan-Meier survival curves were constructed per treatment group. Median survival time for each group was calculated. In the event that an animal's survival time was greater than the time of study termination, the day of study termination was substituted for that animal's survival time and treated as censored in the analysis. Note that the great majority of the animals died before study termination, resulting in very few censored values.

RESULTS

Antibody Conjugate and Radiolabeling

Conjugation of PA-DOTA to HuCC49 and HuCC49ΔCH2 resulted in 3.5 and 3.0 chelates/

Table 1. Conjugation, Labeling, and Binding Parameters

	Specific activity (mCi/mg)[a]	*Chelates/Ab*[b]	K_d *(nM)*[c]
^{177}Lu-PA-DOTA-HuCC49	3.2 (0.5)	3.5	7.4 (1.0)
^{177}Lu-PA-DOTA-HuCC49ΔCH2	3.0 (1.2)	3.0	17.3 (8.5)

[a]Mean with standard deviation in parentheses of six experiments.
[b]Determined by MALDI mass spectrometry.
[c]Mean with standard deviation in parentheses of three experiments.

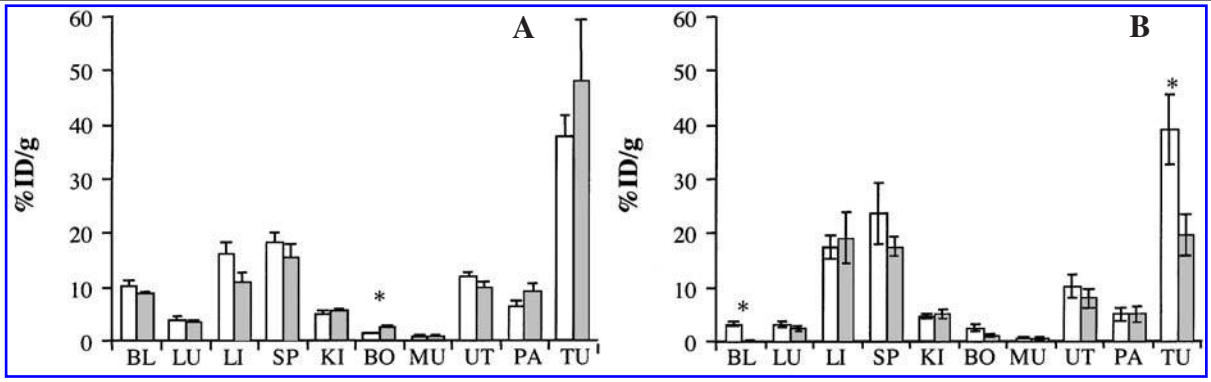

Figure 1. Biodistribution of ^{177}Lu-PA-DOTA-HuCC49 (clear columns) and ^{177}Lu-PA-DOTA-HuCC49ΔCH2 (shaded columns) in mice bearing i.p. LS174T tumors at 4 hours (**A**) and 24 hours (**B**) after (intraperitoneal) i.p. injection of the radiolabeled antibodies. BL, blood; LU, lung; LI, liver; SP, spleen; KI, kidney; BO, bone; MU, muscle; UT, uterus; PA, pancreas; TU, tumor. Each column represents the median tissue concentration from a group of 6–8 animals, with the error bars representing the standard error of the mean. Tissues marked with * show a significant difference ($p < 0.05$) between the uptake of ^{177}Lu-PA-DOTA-HuCC49 and ^{177}Lu-PA-DOTA-HuCC49ΔCH2.

molecule, respectively, as determined by MALDI mass spectrometry.[36] The conjugates were labeled with ^{177}Lu to comparable levels, and competitive inhibition studies estimated similar binding affinity for each molecule (Table 1).

Biodistribution and Pharmacokinetics

Mice bearing LS174T i.p. tumors received i.p. injection of 2 μCi of ^{177}Lu-HuCC49 or ^{177}Lu-HuCC49ΔCH2. At 4 hours postinjection, both targeting molecules had attained high tumor uptake with similar normal tissue uptakes, particularly for the liver, spleen, and urinary tract (Fig. 1A). By 24 hours postinjection, the intact molecule had retained a similar uptake as was present at 4 hours while the ΔCH2 molecule had a significantly lower tumor uptake of 19.3 ± 3.8 %ID/g (Fig. 1B). Furthermore, the intact molecule at 24 hours had 3.2 ± 0.4 %ID/g in the blood while the

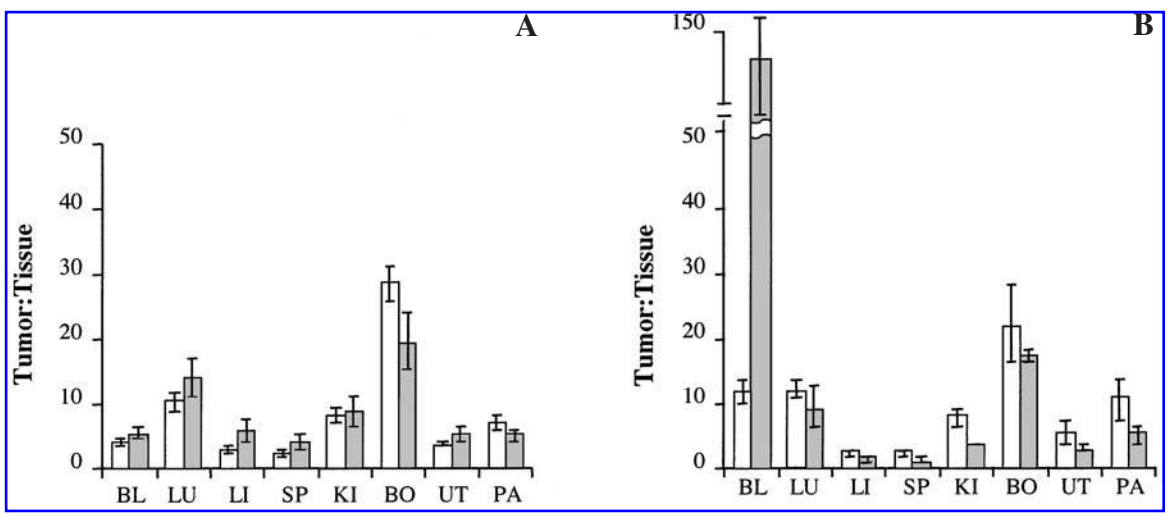

Figure 2. Tumor-to-tissue ratios for ^{177}Lu-PA-DOTA-HuCC49 (clear columns) and ^{177}Lu-PA-DOTA-HuCC49ΔCH2 (shaded columns) in mice bearing i.p. LS174T tumors at 4 hours (**A**) and 24 hours (**B**) after (intraperitoneal) i.p. injection of the radiolabeled antibodies. Each column represents the mean tumor-to-tissue ratio from a group of 6–8 animals, with the error bars representing the standard error of the mean. Abbreviations are defined in Figure 1.

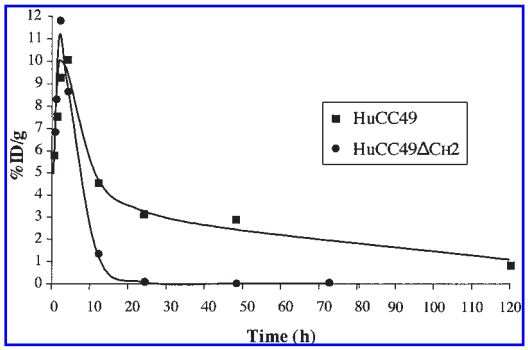

Figure 3. Blood radioactive disappearance curves for ^{177}Lu-HuCC49 and ^{177}Lu-HuCC49ΔCH2.

ΔCH2 molecule had only 0.1 ± 0.03 %ID/g (Fig. 1B). As illustrated in Figure 2, tumor:normal tissue ratios were similar at 4 hours, but at 20 hours, tumor:blood ratios were 5.3 for intact and 144 for the ΔCH2 molecule, reflecting the rapid plasma clearance of the ΔCH2 molecule (Fig. 3). The pharmacokinetic and pharmacodynamic parameters are provided in Table 2. The ΔCH2 molecule had a plasma $T_{1/2}$ of 2.7 hours compared to 61.2 hours for the intact molecule, resulting in a blood AUC that was 17% of the AUC of the intact molecule. In contrast, the ΔCH2 molecule's tumor AUC was 70% of the intact molecule tumor AUC. Thus, the ΔCH2 molecule has a major sparing of the blood/bone marrow radiation exposure while delivering only a modest reduction in tumor radiation. The liver AUC of the ΔCH2 molecule was 31% of the intact molecule while kidney AUC of the ΔCH2 was 29% greater than the intact molecule.

Radiation Dosimetry

Table 3 provides the radiation dose estimates to blood, liver, kidney, and tumor for the ΔCH2 and intact ^{177}Lu-HuCC49 reagents. The ΔCH2 molecule has a 0.023 rad/μCi blood exposure compared to 0.076 rad/μCi for the intact molecule. This reduced blood and marrow exposure should result in a much higher maximal tolerated dose of radiolabeled HuCC49ΔCH2 than the radiolabeled HuCC49. We carried out a maximal tolerated dose (MTD) study and found that the MTD of ^{131}I-HuCC49ΔCH2 was greater than 1100 μCi, as compared to 300 μCi for the ^{131}I-labeled intact molecule. Because ^{177}Lu and ^{131}I have comparable beta energies and physical half-lives, we used ^{131}I to estimate the MTD of HuCC49ΔCH2 and HuCC49. These treatment doses with ^{177}Lu would deliver greater than 1628 cGy and 726 cGy tumor doses through the ΔCH2 and intact molecule, respectively.

Autoradiography

Radial histograms for tumors resected at 1, 4, 24, and 48 hours postinjection are shown in Figure 4. Plotted are the number of voxels in the tumors as a function of radius and dose rate. At 1 hour postinjection, the central tumor regions have lower dose rates, with many voxels experiencing nearly zero dose rates (see Fig. 4A and B). Nearer the surface, the dose rates are much higher, particularly for the ^{177}Lu-PA-DOTA-HuCC49ΔCH2 studies. While the range of dose rates is broad, the average magnitude of the distribution increases and moves away from the zero level. Surface regions display characteristically smaller dose rates giving substantially to asymmetry, the

Table 2. Pharmacokinetics of Intact and ΔCH2 Versions of HuCC49[a]

Tissue	*Conjugate*	C_{max} *(% ID/g)*	T_{max} *(h)*	*AUC (% ID × h/g)*	$T_{1/2ab}$ *(h)*	$T_{1/2el}$ *(h)*
Blood	^{177}Lu-PA-DOTA-HuCC49	11.8	2.3	442.0	0.9	61.2
	^{177}Lu-PA-DOTA-HuCC49ΔCH2	11.2	2.0	73.5	0.8	2.7
Tumor	^{177}Lu-PA-DOTA-HuCC49	41.6	3.3	3760.3	0.5	60.4
	^{177}Lu-PA-DOTA-HuCC49ΔCH2	60.5	7.6	2618.5	1.9	24.1
Liver	^{177}Lu-PA-DOTA-HuCC49	17.6	8.7	4083.8	1.2	155.0
	^{177}Lu-PA-DOTA-HuCC49ΔCH2	19.1	13.2	1286.2	3.6	36.2
Kidney	^{177}Lu-PA-DOTA-HuCC49	3.4	3.3	1364.8	0.7	188.3
	^{177}Lu-PA-DOTA-HuCC49ΔCH2	3.5	7.6	1762.7	0.7	175.6

[a]Pharmacokinetic analysis was performed using a one-compartment bolus model, except for a two-compartment model being used for ^{177}Lu-PA-DOTA-HuCC49 in blood.

Table 3. Radiation Dosimetry (cGy/μCi) for Marrow, Liver, Kidney, and Tumor

	Marrow cGy/μCi	*Liver cGy/μCi*	*Kidney cGy/μCi*	*Tumor cGy/μCi*	*Tumor-to-marrow ratio*
^{177}Lu-PA-DOTA-HuCC49	0.076	1.89	0.35	2.42	31.8
^{177}Lu-PA-DOTA-HuCC49ΔCH2	0.023	1.69	0.40	1.48	64.3

absence of dose from particles originating outside of the tumor. At 4 hours postinjection, dose rates are higher. The ^{177}Lu-PA-DOTA-HuCC49ΔCH2 study still displays higher dose rates near the tumor surface compared to the tumor center or far surface. The ^{177}Lu-PA-DOTA-HuCC49 study displays more uniform dose-rate distributions as a function of radius. At 24 and 48 hours postinjection, dose-rate distributions appear similar for both studies. Dose rates are more uniform than previous times postinjection, including central tumor regions. The broadest range and largest average dose rates are experienced in the region near, but not at, the surface of the tumors. Tumor surfaces have similarly lower dose rates, as expected from asymmetry.

Radioimmunotherapy Studies

We selected a fractionated treatment protocol of 300 μCi i.p. three times daily to illustrate the efficacy of the ^{177}Lu-HuCC49ΔCH2 molecule. As illustrated in Figure 5, the radiolabeled ΔCH2 molecule produced a median survival of 67.5 days as compared to control animals survival of 32 days. The ^{177}Lu-HuCC49 treated animals died of toxicity at a median of 17 days.

DISCUSSION

Murine CC49 mAb labeled with ^{177}Lu has been used for the i.p. treatment of recurrent TAG-72 positive ovarian carcinoma limited to the abdominal cavity in phase I/II clinical trials.[21] Clinical efficacy has been observed in these studies; however, treatment doses were limited owing to bone marrow suppression. In a trial using interferon to increase TAG-72 expression and Taxol® as a radiosensitizing agent in combination with the MTD dose of ^{177}Lu-CC49, there were 4 of 17 (24%) objective responses in patients with measurable disease and 5 of 44 (11%) patients with nonmeasurable disease in remission beyond 2 years. In addition, HAMA responses were observed in all patients, which precluded the repeat administration of radiolabeled murine CC49. To overcome these problems, Slavin-Chiorini et al. produced a humanized, domain-deleted derivative of CC49 (HuCC49ΔCH2).[27] The HuCC49ΔCH2 molecule is designed to have tumor uptake similar to the intact antibody, yet clear more rapidly from the serum, thus reducing hematologic toxicity when radiolabeled. Also, humanization of the construct should lead to a reduced HAMA response when administered to patients. The goal of this study was to evaluate the tumor localization, intratumor distribution, serum clearance, and potential efficacy of HuCC49 and HuCC49ΔCH2 labeled with ^{177}Lu in mice bearing a TAG-72-positive tumor confined to the abdominal cavity.

Previous studies have demonstrated the specific localization of radiolabeled murine CC49 to LS174T tumors.[37] The results of our study indicate that there was greater tumor uptake of ^{177}Lu-PA-DOTA-HuCC49 compared to ^{177}Lu-PA-DOTA-HuCC49ΔCH2 over time, but that ^{177}Lu-PA-DOTA-HuCC49ΔCH2 ($T_{1/2el}$ = 2.7 hours) cleared the blood more rapidly than ^{177}Lu-PA-DOTA-HuCC49 ($T_{1/2el}$ = 61.2 hours). These results are similar to those described by Slavin-Chiorini et al. in which the radioiodinated HuCC49 and HuCC49ΔCH2 had similar uptake in s.c. LS174T tumors at early time points after i.v. or i.p. injection, but at later time points, the HuCC49 uptake was significantly greater than HuCC49ΔCH2.[27] In addition, the radioiodinated HuCC49ΔCH2 cleared from the blood more rapidly than HuCC49 after either an i.v. or an i.p. injection.[27] The uptake and clearance of ^{177}Lu-PA-DOTA-HuCC49 and ^{177}Lu-PA-DOTA-HuCC49ΔCH2 were similar in all other tissues (Figs. 2–4; Table 2).

There has been speculation as to why ΔCH2 molecules clear the serum more quickly than an intact IgG. It is unlikely that the faster clearance is only based on the difference in molecular weight between the two molecules (150 kDa for HuCC49 compared to 124 kDa for HuCC49ΔCH2). Slavin-

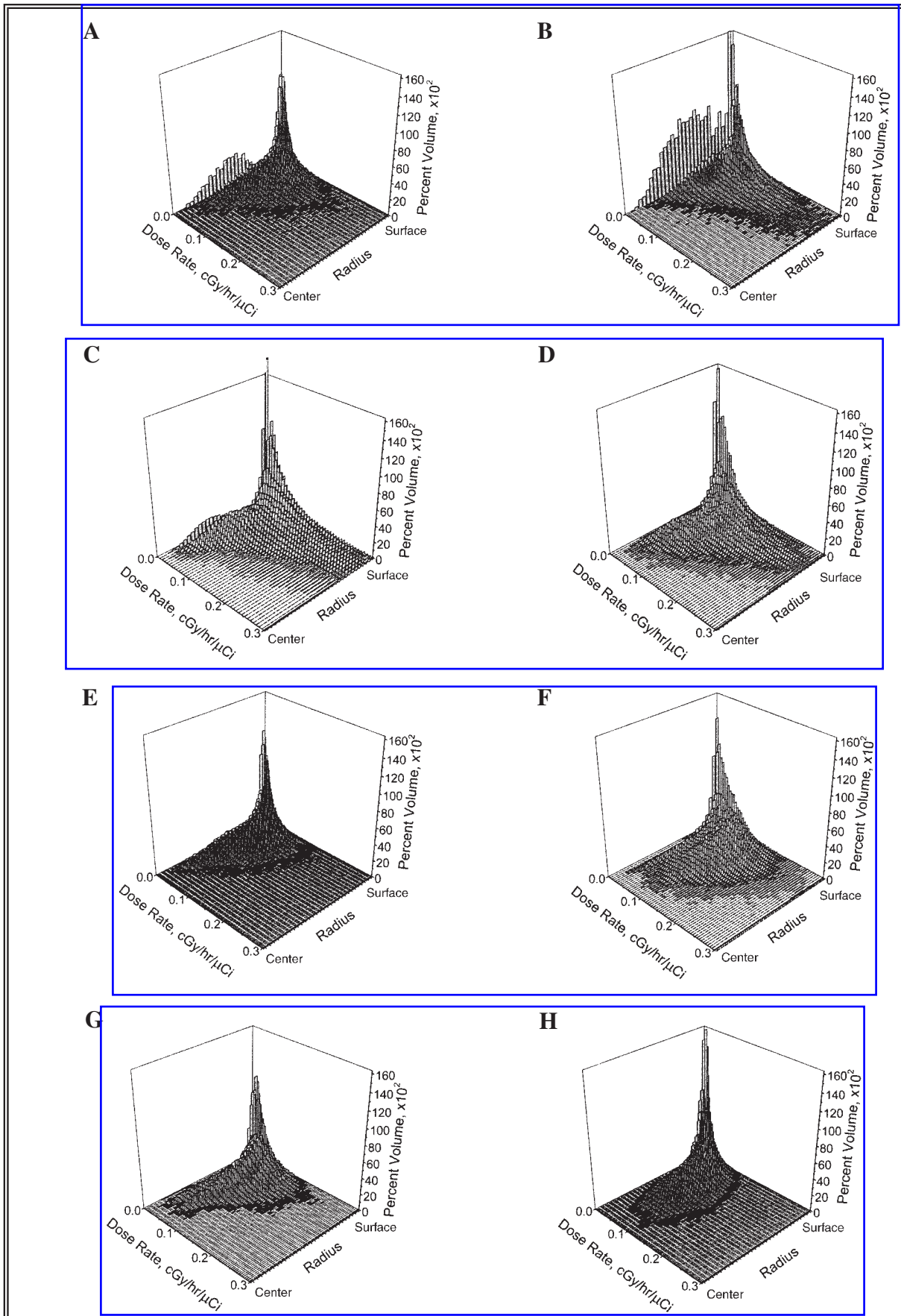

Figure 4. Radial histograms showing the nonuniformity of dose rates at 1, 4, 24, and 48 hours postinjection for ^{177}Lu-PADOTA-HuCC49ΔCH2 (panels A, C, E, G) or ^{177}Lu-PA-DOTA-HuCC49 (panels B, D, F, H), respectively.

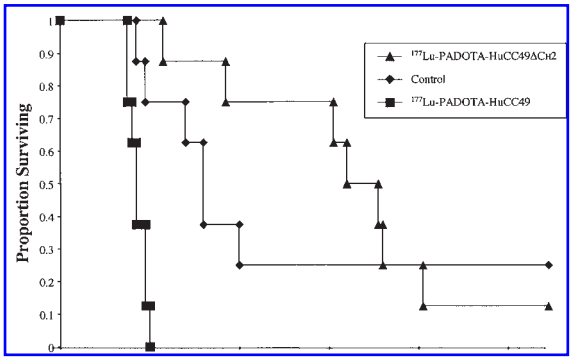

Figure 5. Survival of nude mice bearing peritoneal LS174T tumors injected intraperitoneally (i.p.) with three doses of ^{177}Lu-HuCC49 or ^{177}Lu-HuCC49ΔCH2, 300 μCi dose/animal, on three consecutive days, compared to untreated control animals, with 8 animals/group.

Chiorini et al. suggest that removal of the CH2 region from the mAb prevents it from being cleared by Fc receptors in the liver and allows it to be cleared more quickly through some other mechanism.[27] Future metabolism studies will attempt to determine the mechanism for this more rapid clearance.

Estimated, absorbed radiation doses to the tumor show that 1.6 times more rads can be delivered to the tumor with ^{177}Lu-PA-DOTA-HuCC49 than with ^{177}Lu-PA-DOTA-HuCC49ΔCH2 upon administration of the same amount of radioactivity. However, this would also result in a 3.3-fold greater absorbed radiation dose to the marrow. Because the absorbed radiation dose to the marrow has been the dose-limiting toxicity in human clinical trials, these data suggest that 2–3 times more ^{177}Lu-PA-DOTA-HuCC49ΔCH2 could be administered, leading to a significantly higher absorbed radiation dose to the tumor when compared to ^{177}Lu-PA-DOTA-HuCC49. The MTD of i.p. ^{131}I-PA-DOTA-HuCC49 and ^{131}I-PA-DOTA-HuCC49ΔCH2 was 300 μCi versus greater than 1100 μCi reflecting the short plasma half-life of the ΔCH2 molecule. There are uncertainties in marrow dose estimation using the standard blood method. The blood method assumes no specific uptake of ^{177}Lu-HuCC49 or ^{177}Lu-HuCC49ΔCH2 in marrow. This assumption becomes invalid if marrow has the active uptake of HuCC49, HuCC49ΔCH2, or free ^{177}Lu is recycled into the marrow space after radiopharmaceuticals are metabolized. In this study, HuCC49 and HuCC49ΔCH2 do not bind to marrow. The amount of free ^{177}Lu recycled into marrow space may not be significant because marrow was not visualized above the mouse body background. This is in agreement with the observation that there was no marrow toxicity in the preliminary therapy study with HuCC49ΔCH2.

The nonuniformity of dose and dose rate in tumor is a major concern for radioimmunotherapy. Both the total uptake and nonuniform distribution must be measured to provide a reliable estimate of tumor dosimetry. Some differences in the dose-rate distributions were observed between the ^{177}Lu-PADOTA-HuCC49ΔCH2 and ^{177}Lu-PA-DOTA-HuCC49 studies. At 1 hour postinjection, the higher relative dose rate near the surface for the fragment may be a result of the greater blood concentrations. This may have resulted in greater binding opportunities owing to more rapid molecule movement. The tumor centers show low dose rates for both, indicating that the molecules were localized or were localizing near the blood supply. Significantly higher dose rates at the tumor center for both studies by 4 hours postinjection indicate that the molecules had time to diffuse. As implied by the higher dose rates, the higher blood concentration and tumor uptake at early times for the fragment are concentrated near the tumor surface. This effect may provide two possible therapeutic advantages. A higher local uptake may provide more opportunities for binding, and a higher dose rate would better control the rapidly proliferating cells near the tumor surface. The similarity of the dose-rate distributions at 24 hours and, somewhat, at 48 hours postinjection may be the result of the distribution of antigen sites. A modest advantage in dose-rate uniformity for the fragment is apparent at 48 hours postinjection owing to the relative decline of dose rate near the surface for the intact antibody. Previous fractionated studies with this tumor model[38] concluded that the loss of dose rate near the tumor surface was the dominant effect in tumor recurrence. The most significant result of multiple injections was the ability to increase the dose rate near the tumor surface, prolonging the period of improved dose-rate uniformity. Note that the extreme surface dose rates are lower in both studies owing to the loss of radiation, leaving the tumor volume and the lack of uptake outside of the tumor to compensate for the loss (geometrical effect). This geometrical effect is less apparent than for other radionuclides owing to the low penetrating power of the ^{177}Lu beta spectrum.

A likely interpretation of the 3-D dose-rate distributions is that the increased initial blood con-

centrations present in the fragment study increased binding near the tumor surface where the blood supply feeds the rapidly proliferating cells. The increased concentrations, to a lesser extent, contributed to diffusion to the tumor interior, balancing the competing effects of increased local binding and diffusion to more distant locations. This resulted in modestly more uniform dose-rate distributions at later times (e.g., 48 hours postinjection) for the fragment study.

The pharmacokinetics and dosimetry studies suggested that higher doses of the ^{177}Lu-HuCC49ΔC_H2 would be better tolerated and more efficacious than the ^{177}Lu-HuCC49. Our preliminary therapy study illustrated these dose effects with the radiolabeled ΔC_H2 molecule mediating efficacy with no toxicity. Other strategies to enhance survival include the administration of interferon to increase TAG-72 expression, dose fractionation, and the use of a radiosensitizer, such as Taxol®. These studies support the concept that i.p. radioimmunotherapy with ^{177}Lu or other radiolabeled HuCC49ΔC_H2 should allow higher therapeutic doses to be administered with reduced immunogenicity and improved efficacy in patients with i.p. ovarian cancer and potentially other tumors, such as mesothelioma and pseudomyxoma peritonei.

CONCLUSIONS

^{177}Lu-PA-DOTA-HuCC49ΔC_H2 appears promising for the treatment of i.p. disease because of the high tumor uptake and rapid blood clearance, which would allow for higher total radionuclide doses to be administered than with ^{177}Lu-PA-DOTA-HuCC49.

ACKNOWLEDGMENTS

We thank Sheila Bright, Synethia Kidd, Christine Olsen, and Kristi Schmitt for their expert technical assistance.

REFERENCES

1. Bischof Delaloye A. Radioimmunoimaging and radioimmunotherapy: Will these be routine procedures? *Semin Nucl Med* 2000;30:186.
2. Knox SJ, Meredith RF. Clinical radioimmunotherapy. *Semin Radiat Oncol* 2000;10:73.
3. Goldenberg DM. Targeted therapy of cancer with radiolabeled antibodies. *J Nucl Med* 2002;43:693.
4. Jhanwar YS, Divgi C. Current status of therapy of solid tumors. *J Nucl Med* 2005;46(Suppl. 1):141S.
5. Sharkey RM, Goldenberg DM. Perspectives on cancer therapy with radiolabeled monoclonal antibodies. *J Nucl Med* 2005;46(Suppl 1):115S.
6. LoBuglio AF, Wheeler RH, Trang J, et al. Mouse/human chimeric monoclonal antibody in man: Kinetics and immune response. *Proc Natl Acad Sci USA* 1989;86:4220.
7. Meredith RF, LoBuglio AF, Plott WE, et al. Pharmacokinetics, immune response, and biodistribution of iodine-^{131}-labeled chimeric mouse/human IgGI, 17-1A monoclonal antibody. *J Nucl Med* 1991;32:1162.
8. Buchegger F, Pelegrin A, Delaloye B, et al. Iodine-^{131}-labeled MAb F(ab′)$_2$ fragments are more efficient and less toxic than intact anti-CEA antibodies in radioimmunotherapy of large human colon carcinoma grafted in nude mice. *J Nucl Med* 1990;31:1035.
9. Adams GP, Schier R, Marshall K, et al. Increased affinity leads to improved selective tumor delivery of single-chain Fv antibodies. *Cancer Res* 1998;58:485.
10. Pavlinkova G, Booth BJ, Batra SK, et al. Radioimmunotherapy of human colon cancer xenografts using a dimeric single-chain Fv antibody construct. *Clin Cancer Res* 1999;5:2613.
11. Goel A, Colcher D, Baranowska-Kortylewicz J, et al. Genetically engineered tetravalent single-chain Fv of the pancarcinoma monoclonal antibody CC49: Improved biodistribution and potential for therapeutic application. *Cancer Res* 2000;60:6964.
12. Fujimori K, Covell DG, Fletcher JE, et al. A modeling analysis of monoclonal antibody percolation through tumors: A binding-site barrier. *J Nucl Med* 1990;31:1191.
13. Yokota T, Milenic DE, Whitlow M, et al. Rapid tumor penetration of a single-chain Fv and comparison with other immunoglobulin forms. *Cancer Res* 1992;52: 3402.
14. Adams GP, Schier R, McCall AM, et al. High affinity restricts the localization and tumor penetration of single-chain fv antibody molecules. *Cancer Res* 2001;61: 4750.
15. Slavin-Chiorini DC, Kashmiri SVS, Schlom J, et al. Biological properties of chimeric domain-deleted anticarcinoma immunoglobulins. *Cancer Res (Suppl),*1995; 55:5957S.
16. Johnson VG, Schlom J, Paterson AJ, et al. Analysis of a human tumor-associated glycoprotein (TAG-72) identified by monoclonal antibody B72.3. *Cancer Res* 1986; 46:850.
17. Thor A, Gorstein F, Ohuchi N, et al. Tumor-associated glycoprotein (TAG-72) in ovarian carciomas defined by monoclonal antibody B72.3. *J Natl Cancer Inst* 1986; 76:995.
18. Murray JL, Macey DJ, Grant EJ, et al. Phase II trial of ^{131}I-CC49 Mab plus alpha interferon (rlFNα) in breast cancer. *J Immunother* 1994;16:162.

19. Murray JL, Macey DJ, Kasi LP, et al. Phase II radioimmunotherapy trial with ^{131}I-CC49 in colorectal cancer. *Cancer (Suppl)* 1994;73:1057.
20. Mulligan T, Carrasquillo JA, Chung Y, et al. Phase I study of intravenous ^{177}Lu-labeled CC49 murine monoclonal antibody in patients with advanced adenocarcinoma. *Clin Cancer Res* 1995;1:1447.
21. Alvarez RD, Partridge EE, Khazaeli MB, et al.. Intraperitoneal radioimmunotherapy of ovarian cancer with ^{177}Lu-CC49: A phase I/II study. *Gynecol Oncol* 1997;65:94.
22. Tempero M, Leichner P, Dalrymple G, et al. High-dose therapy with iodine-^{131}-labeled monoclonal antibody CC49 in patients with gastrointestinal cancers: A phase I trial. *J Clin Oncol* 1997;15:1518.
23. Tempero M, Leichner P, Baranowska-Kortylewicz J, et al. High-dose therapy with ^{90}Yttrium-labeled monoclonal antibody CC49: A phase I trial. *Clin Cancer Res* 2000;6:3095.
24. Meredith RF, Alvarez RD, Partridge EE, et al. Intraperitoneal radioimmunochemotherapy of ovarian cancer: A phase I study. *Cancer Biother Radiopharm* 2001;16:305.
25. Maraveyas A, Epenetos AA. Radioimmunotherapy of ovarian cancer. In: Goldenberg DM, ed. *Cancer Therapy with Radiolabeled Antibodies*. Boca Raton, FL: CRC Press, 1995:155.
26. Kashmiri SVS, Shu L, Padlan EA, et al. Generation, characterization, and *in vivo* studies of humanized anticarcinoma antibody CC49. *Hybridoma* 1995;14:461.
27. Slavin-Chiorini DC, Kashmiri SVS, Lee H-S, et al. A CDR-grafted (humanized) domain-deleted antitumor antibody. *Cancer Biother Radiopharm* 1997;12:305.
28. Buchsbaum DJ, Rogers BE, Khazaeli MB, et al. Targeting strategies for cancer radiotherapy. *Clin Cancer Res* 1999;5(Suppl.):3048S.
29. Chappell LL, Rogers BE, Khazaeli MB, et al. Improved synthesis of the bifunctional chelating agent 1,4,7, 10-tetraaza-*N*-(1-carboxy-3-(4-nitrophenyl)propyl)-*N′*, *N″*, *N‴-tris* (acetic acid)cyclododecane (PA-DOTA). *Bioorg Med Chem* 1999;7:2313.
30. *SAS/STAT User's Guide, Version 6*, 4th. ed. Cary, NC: SAS Institute Inc., 1989.
31. Roberson PL, Heidorn DB, Kessler ML, et al. Three-dimensional reconstruction of monoclonal antibody uptake in tumor and calculation of beta dose-rate nonuniformity. *Cancer* 1994;73:912.
32. Siegel JA, Wessels BW, Watson EE, et al. Bone marrow dosimetry and toxicity for radioimmunotherapy. *Antibody Immunoconj Radiopharm* 1990;3:213.
33. Epp ER, Woodard HQ, Weiss H. Energy absorption by the bone marrow of the mouse receiving whole-body irradiation with 250-Kv X-rays or cobalt-60 gamma rays. *Radiat Res* 1959;11:184.
34. Muthuswamy MS, Roberson PL, Buchsbaum DJ. A mouse bone marrow dosimetry model. *J Nucl Med* 1998;39:1243.
35. Berger MJ. Distribution of absorbed dose around point sources of electrons and beta particles in water and other media. MIRD No. 7. *J Nucl Med* 1971;12 (Suppl. 5):5.
36. Hollander M, Wolfe DA. *Nonparametric Statistical Methods*, 2nd ed. New York, NY: John Wiley & Sons, 1999.
37. Safavy A, Khazaeli MB, Kirk M, et al. Further studies on the protein conjugation of hydoxamic acid bifunctional chelating agents: Group-specific conjugation at two different loci. *Bioconjug Chem* 1999;10:18.
38. Roberson PL, Dudek S, Buchsbaum DJ. Dosimetric comparison of bolus and continuous injections of CC49 monoclonal antibody in a colon cancer xenograft model. *Cancer (Suppl),* 1997;80:2567.